NON-LINEAR PHENOMENA ANALYSIS AND CHAOS PREDICTION OF STALL-INDUCED AEROELASTIC OSCILLATIONS VIA LYAPUNOV EXPONENTS

Flávio D. Marques, Andréia R. Simoni, Vilma A. Oliveira
Engineering School of São Carlos - University of São Paulo, São Carlos, Brazil

Keywords: *space state reconstruction, aeroelasticity, nonlinear systems, chaos*

Abstract

The analysis of non-linear dynamical systems can be based on data from either a mathematical model or an experiment. Mathematical models for aeroelastic response associated to the dynamic stall behaviour are very hard to obtain. In this case, experimental or flight data seems to provide a more suitable basis for non-linear dynamical analysis. Dynamic systems techniques based on time series analysis can be adequately applied to non-linear aeroelasticity. When experimental data are available, state space reconstruction methods have been widely considered. Moreover, the Lyapunov exponents provides qualitative and quantitative characterization of nonlinear systems chaotic behavior. A positive Lyapunov exponent is a strong signature of chaos. This work presents the application of Lyapunov exponents calculation for nonlinear aeroelastic responses, in order to predict chaotic behavior. State space reconstruction has been also performed by means of the method of delays. An aeroelastic wing model has been constructed and tested in a closed circuit wind tunnel. The wing model has been mounted on a turntable that allows variations in the wing incidence angle. Structural deformation is captured by means of strain gages thereby providing information on the aeroelastic response. The method of delays has been used to identify an embedded attractor in the state space from experimentally acquired aeroelastic response time series. To obtain the time delay value to manipulate the time series during reconstruction, the autocorrelation function analysis has been used. For the attractor embeeding dimension calculation the correlation integral approach has been considered. To predict positive Lyapunov exponent two methods have been considered. Data filtering has been aldo considered and the effects on Lyapunov exponents calculation are discussed. This preliminary work has been successful in predicting chaotic structures from aeroelastic time series. Future applications are towards robust methodologies that can provide better physical interpretation on chaos in aeroelastic systems.

1 Introduction

The treatment of aeroelastic phenomena with linear models have provided a reasonable amount of tools to the assessment and analysis of most of the adverse behaviour [1], [2]. Nonetheless, modern aviation has shown advances that lead to lighter and faster aircraft, thereby increasing the danger for severe aeroelastic problems. For instance, transonic flight is surrounded by a complex mixture of flows experiencing different speeds, aggravated by shock waves appearance. Aeroelastic phenomena associated to those compressibility effects introduce a great deal of nonlinear effects, and can not be predicted with linear models [3]. Highly separated flows also lead to complex aeroelastic phenomena that are difficult to model [4].

Non-linear aeroelasticity research has re-

cently become more relevant. Various approaches have been taken to model non-linear aeroelastic behaviour. In some cases the complex unsteady aerodynamics has been resolved with CFD methods [3], or by other methodologies to reduce the computational effort [4], [5]. However, the majority of non-linear aeroelastic models still need to be validated or checked. In this case, experimental data is of great importance, but it is not common to find significant non-linear aeroelastic data available.

Among the possible behaviour that a non-linear system presents one can assess are many equilibrium points, bifurcations, limit cycles, chaos, etc. Bifurcations and limit cycles occur mainly in transonic aeroelastic responses or when introducing non-linear structural dynamics [6]. Moreover, chaotic motion almost certainly appears in highly separated flows, such as the case of dynamic stall [7].

The analysis of non-linear dynamical systems can be based on data from either a mathematical model or an experiment. A variety of mathematical tools have been available to explore and analyse such possible non-linear features, which can also be applied to aeroelastic problems [8]. Mathematical models for aeroelastic response associated to the dynamic stall behaviour or stall-induced motion are very hard to obtain. In this case, experimental or flight data seems to provide a more suitable basis for non-linear dynamical analysis. Experimental data furnishes a sequence of measurements that corresponds to a time series with the embedded system dynamics.

Typical dynamical systems responses can be assessed by means of reconstructing the state space from time series using the so-called method of delays (MOD). This technique has been shown to be robust enough to characterize non-linear dynamic systems, as well as to analyze chaotic behaviour. The fundamentals of this method have been introduced by Packard [9] and Takens [10]. The MOD uses delayed values of the time series to build a new coordinate system. This leads to the reconstruction of the state space for the observed dynamical system and any embedding attractor of interest in the true state space can be reconstructed. The main task of the MOD is then to provide adequate values for the time delays and the so-called embedding dimension (attractor dimension). Several approaches to obtain the MOD parameters have been investigated. The aim of this paper is to present techniques from the theory of non-linear time series analysis for the investigation of experimentally acquired non-linear aeroelastic phenomena. The characterization of the non-linear behaviour of stall-induced oscillations of an aeroelastic wing is achieved using the method of delays, leading to the state space reconstruction. An aeroelastic wing model has been constructed and tested in a wind tunnel. The wing model has been mounted on a turntable that allows variations in its incidence angle. Structural deformation is captured by means of strain gages, thereby providing information on the aeroelastic responses. The test cases correspond to aeroelastic response time series at specific strain gages points due to oscillatory motions of the turntable. A self-sustained oscillatory motion observed when the turntable is left free to move in the flow field, is also considered for analysis. The parameters for applying the method of delays are the time delay and the embedding (attractor) dimension. The autocorrelation function has been used to determine the time delays, while the correlation integral is used to obtain the embedding dimension. Evolutions of reconstructed state spaces, with respect to flow and motion parameters, are presented and discussed. Two methods based on reconstructed spaces have been considered to seatch for positive Lyapunov exponents and the comparative results are presented.

2 State space reconstruction

Consider a dynamical system

$$\mathbf{x}(k+1) = \mathbf{F}(\mathbf{x}(k)) \tag{1}$$

where $\mathbf{x}$ and $\mathbf{F}$ are n-dimensional vectors. The embedding theorem attributed to Takens [10] and Mañé [11], established that if one is able to observe a single scalar quantity, say $h(\cdot)$, of some function $g(\mathbf{x}(k))$ then the geometric structure of

the system dynamics can be unfolded from this set of scalar measurements $h(g(\mathbf{x}(k))$ in a space made out of new vector

$$\begin{aligned}\mathbf{y}_k &= [h(\mathbf{x}(k))\ h(g^1(\mathbf{x}(k)))\ h(g^2(\mathbf{x}(k)))\ \dots \\ &\quad h(g^{\mathrm{T}d-1}(\mathbf{x}(k)))]^{\mathrm{T}} \end{aligned} \tag{2}$$

which define motion in a d-dimensional space [12]. If d is large enough, for smooth functions $h(\cdot)$ and $g(\cdot)$ it is shown that many important properties of $\mathbf{x}(k)$ are reproduced in the new space given by $\mathbf{y}_k$ without ambiguity [13].

Let $s(k)$ denote the actual measured variable. If one choose $h(\cdot)$=$s(k)$ and $g^i(\mathbf{x}(k)) = \mathbf{x}(k+T_i) = \mathbf{x}(t_0+(k+T_i)\tau_s)$ with τ_s being the sampling time, the new vector for $T_i = iT$ takes the form

$$\begin{aligned}\mathbf{y}_k &= [s(k)\ s(k+T)\ s(k+2T)\ \dots \\ &\quad s(k+T(d-1)]^{\mathrm{T}}. \end{aligned} \tag{3}$$

The space constructed by using the vectors $\mathbf{y}_k$ is called the reconstructed space, the parameter T is called time delay and d the embedded dimension. According to the theory of state space reconstruction, the geometric structure of an attractor can be observed in the d-dimensional reconstructed space if $d \geq 2d_a + 1$, with d_a the dimension of the attractor of interest. The central issue in the reconstruction of the state space is the choice of the time lag $T\tau_s$ along with the dimension d.

The time lag $T\tau_s$ is usually chosen as the quarter of the period of the predominant frequency in the Fourier spectrum of the measured variable or equivalently T is found as the first zero of the linear autocorrelation function

$$C(T) = \sum_k [s(k) - \bar{s}][s(k+T) - \bar{s}] \tag{4}$$

where $\bar{s} = \frac{1}{N_0}\sum_{k=1}^{N_0} s(k)$ with N_0 is the total number of sampled points.

There are different methodologies to assess the embedding dimension. When dynamical system responses are obtained from experiments, noise contamination is practically inevitable. The determination of the MOD parameters must follow specific procedures in order to guarantee proper state space reconstruction. The methodology considered here uses the saturation of system invariants, that is, the invariance properties of an attractor calculated from the reconstructed trajectory does not change by increasing d. To estimate d, the average fraction of the number of points on the attractor with interdistances less than r are calculated from the correlation integral $C(r)$ [8]:

$$C^d(r) = \frac{1}{M^2}\sum_{\substack{i,j=0 \\ i\neq j}}^{M} H(r - |\mathbf{y}_i - \mathbf{y}_j|) \tag{5}$$

where $M = N_0 - T(d-1)$ and $H(t)$ is the Heaviside function, that is:

$$H(u) = \begin{cases} 1 & \text{if } u \geq 0 \\ 0 & \text{if } u < 0 \end{cases}. \tag{6}$$

The $|\cdot|$ is taken as the Euclidean distance

$$|\mathbf{y}_i - \mathbf{y}_j| = \sqrt{\sum_{k=1}^{d} (s_{i+T(k-1)} - s_{j+T(k-1)})^2}. \tag{7}$$

The correlation integral $C^d(r)$ is a function of r and the embedding dimension d. The slope of $\log_{10} C^d(r)$ versus $\log_{10} r$ is calculated as a function of d over a sufficient range for small interdistances r and the embedding dimension d is thus obtained when the slope becomes independent of d. The slope tends to saturate into a value called the correlation dimension.

3 Lyapunov exponents

The Lyapunov exponents are essentially a measure of the average rates of expansion and contraction of point in trajectories in phase space. They are asymptotic quantities, defined locally in state space, describing the exponential rate at which a perturbation to a trajectory of a system grows or decays with time at a certain location in the state space [8].

Given a continuous dynamical system in an n-dimensional phase space, the Lyapunov exponents can be monitored in terms of the long-term evolution of an infinitesimal n-sphere of inicial conditions. The infinitesimal n-sphere will become an n-ellipsoid due to the locally deforming nature of the flow [14]. The i^{th} one-dimensional Lyapunov exponent is them defined in terms of the length of the ellipsoidal principal axis $p_i(t)$:

$$\lambda_i = \lim_{t\to\infty} \frac{1}{t} \log_2 \frac{p_i(t)}{p_i(0)}$$

where the λ_i are ordered from largest to smallest.

The Lyapunov exponents signs provide a qualitative picture of a system dynamics. In a three-dimensional continuous dissipative dynamical system the only possible spectra, and the attractors can be described as: $(+,0,-)$, a strange attractor; $(0,0,-)$, a two-torus; $(0,-,-)$, a limite cycle; and $(-,-,-)$, a fixed point [14].

4 Experimental Apparatus and Database

The aeroelastic wing comprises a wind tunnel model of an arbitrary straight rectangular semi-span wing. The wind tunnel facility presents a testing chamber with about $2m^2$ cross-section area. The maximum flow speed in the testing chamber is $50\frac{m}{s}$ with turbulence level of 0.3%. The wing model has been fixed to a turntable that allows incidence variation to the wing. The wing semi-span is $800mm$ and the chord is $290mm$.

The model main structure has been constructed using fiber glass and epoxy resin in the shape of a tapered plate. The taper ratio is of $1:1.67$, where the width at the wing root is $250mm$. To provide aerodynamic shape high density foam and wooden cover have been used. The NACA0012 airfoil from wing's root to tip has been used. In order to minimize as much as possible the effects of the skin to the wing structure stiffness, both foam and wooden shell have been segmented at each $100mm$ spanwise.

Figure 1 illustrates the experimental apparatus with indications of the strain gages locations inside the wing model.

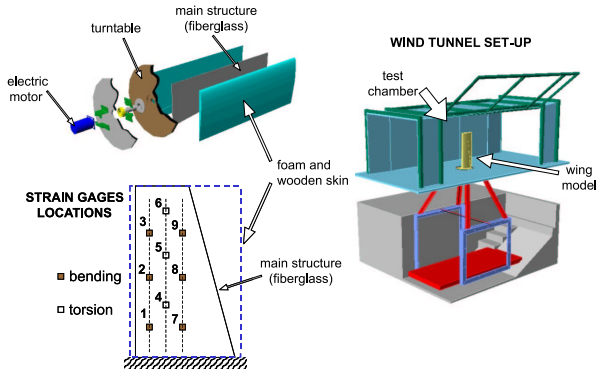

Fig. 1 Experimental set-up and strain gages locations.

Incidence motion is achieved with an electrical motor mounted beneath the turntable. The motor actions are controlled by software integrated to the acquisition system. Strain gages have been fixed to the plate surface to furnish proper measurement of the dynamic response of the wing main structure. The strain gages have been distributed along three lines spanwise. The first and last lines present three strain gages each, all to capture bending motions. The intermediate line presents three strain gages for torsional motion.

Data acquisition and the motion control of the servo motor have been achieved by using a dSPACE® DS1103 PPC controller board and real-time interface for SIMULINK®. The HBM® KWS 3073 amplifier for strain gage bridge energizing has been used to acquire and amplify the strain gage signals. The resulting signals are directly acquired by the dSPACE® controller board, allowing subsequent data storage into a PC compatible computer.

5 Results and Discussion

During experiments different turntable motions have been executed and the respective aeroelastic responses at each strain gage point have been acquired. Prescribed turntable motions correspond to oscillatory and random ones, and they have been also carried out at different airspeeds (from 9 to 16.5 $\frac{m}{s}$, approximately). Oscillatory motions

have been run at relatively low amplitude values (maximum of 5.5°), but such oscillations have been considered around two average angles, that is, zero and 9.5°. For the cases where the average oscillatory angle is about 9.5°, highly unsteady separated flow is occuring. These cases furnish an adequate database for non-linear phenomena investigation.

The randomly generated motions follow the same strategy. Tests have been also proceeded for static turntable at different incidences and for free turntable at a range of flow speeds. For the last one, it has been observed a peculiar self-sustained oscillatory motion at higher angles of attack.

The techniques for assessing the time delay and embedding dimension have been used to provide the basic parameters for state space reconstruction. Figure 2 shows the time delay determination by means of the autocorrelation function. The time delay is taking where the autocorrelation function becomes zero. Figure 3 illustrates the embedding dimension determination via the analysis of the correlation integral and its saturation as the dimension increases. Saturation can be observed when the curves of $\log_{10} C^d(r)$ versus $\log_{10} r$ for each dimension present a similarity in their slopes.

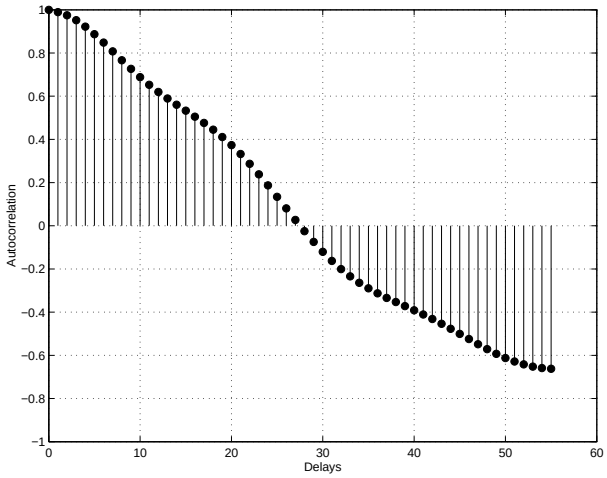

Fig. 2 Time delay determination.

State space reconstruction has been achieved and the non-negative Lyapunov exponent was

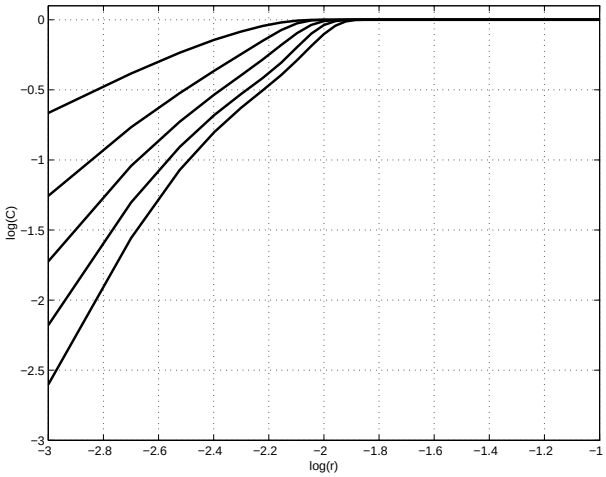

Fig. 3 Embedding dimension determination.

calculated for stall-induced aeroelastic responses when the turntable is free to move.

When the turntable is left free, the aerodynamic forces and other flow effects are the responsable for the wing motion. It has been observed a peculiar self-sustained oscillatory motion of the wing, typical of a limit cycle. The oscillatory motion has kept the amplitude confined in between 4.0° to 14.0° turntable incidence angle. In these cases the stall has induced a deep break to the increasing pitching moment that builds up for the free wing motion immerse into the flow. Both incidence angle and frequencies increase as flow speed also increases.

The torsional measurement time series, that has been acquired from the strain gage at the point 4 (Fig. 1), has been used to reconstruct the state space. The experiments have been carried out for six different freestream velocities and the resulting time delays for these cases are summarized in the Tab. 1, where U_∞ is the freestream velocity. The embedding dimension is found to be 3, which leads to the reconstructed vectors as $\mathbf{y}_k = [x(k)\ x(k+T)\ x(k+2T)]^{\mathrm{T}}$.

Figure 4 shows the evolution in terms of freestream velocity of the reconstructed state spaces. Periodic motion is evident from the obtained trajectories. The bouncing phenomenon is also observed in these cases, which characterizes the existence of a resonance mode. The effect of

Table 1 Parameters for free turntable.

Case	$U_\infty(\frac{m}{s})$	time delay
1	9.42	27
2	11.46	24
3	13.49	22
4	14.29	21
5	15.13	20
6	16.75	18

stall inducing the breakdown in pitching moment may be the reason for such phenomenon. The reconstructed state spaces depict a closed orbit that corresponds to a limit cycle.

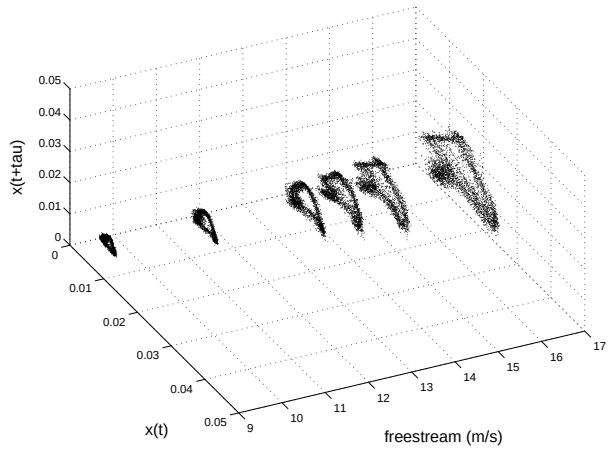

Fig. 4 Evolution with respect to the freestream velocity of reconstructed state spaces for free turntable cases.

Figure 5 presents the reconstructed state space without low pass filtering and Fig. 6 presents the reconstructed state space with low pass filtering for the case 5 for free turntable (Tab. 1).

Since a positive maximal Lyapunov exponent is a strong signature of chaos, it is of considerable interest to determine its value for a given time series [15]. The first algorithm for this purpose was suggested by Wolf et al [14]. Table 2 presents the Lyapunov exponents obtained for the case 5 in free turntable with and without filtering using

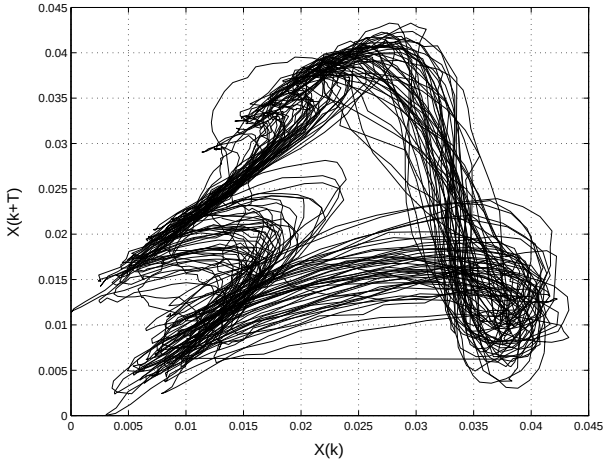

Fig. 5 Reconstructed space state for case 5 without low pass filtering.

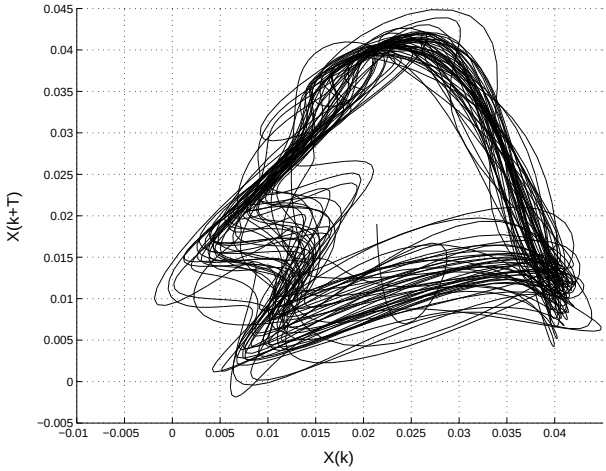

Fig. 6 Reconstructed space state for case 5 with low pass filtering.

the method proposed by Wolf et al[14].

Table 2 Lyapunov exponents obtained using the method by Wolf et al [14]

	Lyapunov Exponents
without filtering	0.34441
with filtering	0.31661

The method proposed by Wolf et al [14] is efficient to characterize the chaotic behaviour, but it is limited to the non-negative Lyapunov expo-

nent and it is impossible calculate the other system's invariants. Moreover, this algorithm does not allow one to test for the presence of exponential divergence, but just assumes its existence and thus yields a finite exponent for stochastic data also, where the true exponent is infinite [15].

Rosenstein et al. [16] and Kantz [17] had developed independently, similar algorithms based in the Wolf's algorithm. In these works they consider that the divergence between nearby trajectories in a determinated direction oscillates through the sinal. It tests directly for the exponencial divergence and thus allows us to decide whether it really makes sense to compute a Lyapunov exponent for a given data set. This algorithm allows to calculate the other invariants of the system. It seems to be adjusted in the calculation of the Lyapunov exponents in time series.

The Lyapunov exponent have been obtained using the method proposed by Roseinstein et al [16]. Table 3 presents the Lyapunov exponents obtained for the case 5 in free turntable with and without filtering.

Table 3 Lyapunov exponents obtained using the method by Rosenstein et al [16]

	Lyapunov Exponents
without filtering	0.34405
with filtering	0.52764

In the Wolf's method [14], if the data are noisy it is important that the initial distance between the reference trajectory and a new neighbour are larger than the noise level, otherwise fluctuations due to noise would be interpreted as deterministic divergence [17].

Another drawback is that the embedding dimension is an important parameter. For small dimension values, the trajectories may diverge simply because they are not neighbours in the true phase space.

The choice of the time delay and replacement steps is also very important to calculate of the Lyapunov exponents. The choice of the replacement steps depends on additional parameters. Accurate exponent calculation therefore requires the consideration of the following interrelated points: the desirability of maximizing evolution times, the tradeoff between minimizing replacement vector size and minimizing the concomitant orientation error, and the manner in which orientation errors can be expected to accumulate.

Finally, in none of the two methods the filtering has modified the nature of the results. The positive exponents obtained by the two methods, indicate the presence of chaos. However, the different results between the methods will be studied on going research.

6 Concluding Remarks

Techniques from the theory of time series analysis, in the context of non-linear systems, is used to investigate experimentally acquired nonlinear aeroelastic phenomena. An aeroelastic wing model has been tested in wind tunnel. Aeroelastic responses have been obtained from strain gages outputs. The wing is mounted on a turntable that allows variations to the incidence angle. The aeroelastic time series are related to oscillatory and free turntable motions. The aeroelastic responses studied in this paper are influenced by highly separated flow fields. The method of delays is employed and for the oscillatory turntable motion a complex evolution of the reconstructed state space is observed when reduced frequency varies for the same freestream velocity. It is possible to infer that bifurcation and chaotic behaviour are related to the aeroelastic system. It has been observed that when the turntable is left free in the aerodynamic flow, a self-sustained oscillation happens. In this case, the existence of the bouncing phenomenon, characterizing a resonance mode, is observed. The reconstructed attractors depict a closed orbit corresponding to a limit cycle. The non-negative Lyapunov exponents obtained by two different methods indicate the occurrence of chaos.

References

[1] P. P. Friedmann. The renaissance of aeroelasticity and its future. In *Proceedings of the International Forum on Aeroelasticity and Structural Dynamics, CEAS 97*, volume 1, pages 19–49, Roma, Itália, 17-20 Junho 1997.

[2] I. E. Garrick. Aeroelasticity - frontiers and beyond. *Journal of Aircraft*, 13(9):641–657, 1976.

[3] J. W. Edwards. Computational aeroelasticity. In A. K. Noor and S. L. Vemuri, editors, *Structural Dynamics and Aeroelasticity*, volume 5 of *Flight-Vehicle Materials, Structures, and Dynamics - Assessment and Future Directions*, pages 393–436. ASME, 1993.

[4] J. G. Leishman and T. S. Beddoes. A semi-empirical model for dynamic stall. *Journal of the American Helicopter Society*, 34:3–17, 1989.

[5] F. D. Marques. *Multi-Layer Functional Approximation of Non-Linear Unsteady Aerodynamic Response*. PhD thesis, University of Glasgow, Glasgow, UK, 1997.

[6] H. Alighanbari and S. J. Price. The post-hopf-bifurcation response of an airfoil in incompressible two-dimensional flow. *Nonlinear Dynamics*, 10:381–400, 1996.

[7] L. E. Ericsson and J. P. Reding. Dynamic stall at high frequency an large amplitude. *Journal of Aircraft*, 17:136–142, 1980.

[8] A. H. Nayfeh and B. Balachandran. *Applied Nonlinear Dynamics*. John Wiley & Sons, New York, 1995.

[9] N. H. Packard, J. D. Farmer, J. P. Crutchfield, and R. S. Shaw. Geometry of time series. *Physical Review Letters*, 45(9):712–716, 1980.

[10] F. Takens. Detecting strange attractors in turbulence. In D. Hand and L.S. Young, editors, *Dynamical Systems and Turbulence*, pages 366–381. Springer, 1981.

[11] R. Mañé. On the dimension of compact invariant sets of certain nonlinear maps. In D. Hand and L. S. Young, editors, *Dynamical Systems and Turbulence*, pages 230–242. Springer, 1981.

[12] H. D. I. Abarbanel. *Analysis of Observed Chaotic Data*. Springer-Verlag, New York, 1996.

[13] T. Sauer, J. A. Yorke, and M. Casdalgi. Embedology. *Journal of Statistical Physics*, 65:579–616, 1991.

[14] A. Wolf, J. B. Swift, H. L. Swinney, and J. A. Vastano. Determining lyapunov exponents from a time series. *Physica D*, 16:285–317, 1985.

[15] H. Kantz and T. Schreiber. *Nonlinear Time Series Analysis*. Cambridge University Press, Cambridge, 2000.

[16] M. T. Rosenstein, J. J. Collins, and C. J. Deluca. A practical method for calculating largest lyapunov exponents from small data sets. *Physica D*, 65(1-2):117 – 134, 1993.

[17] H. Kantz. A robust method to estimate the maximal lyapunov exponent of a time-series. *Physics Letters A*, 185(1):77 – 87, 1994.